Physica Scripta. Vol. 3, 125–132, 1971

Lifetime Measurements in Si II, Si III, and Si IV

H. G. Berry,[1] J. Bromander, L. J. Curtis[2] and R. Buchta

Research Institute for Physics, Stockholm, Sweden

Received April 16, 1971

Abstract

Lifetime measurements in Si II, Si III, and Si IV. H. G. Berry, J. Bromander, L. J. Curtis and R. Buchta (Research Institute for Physics, 10 405 Stockholm 50, Sweden).
Physica Scripta (*Sweden*) *3*, 125–132, 1971.

We have measured radiative decay times in Si II, Si III, and Si IV in the wavelength region 700–6 000 Å using the beam-foil technique. The lifetimes and transition probabilities have been evaluated by alternative methods of curve-fitting and cascade analysis. These results are compared with theoretical transition probabilities, and values in other members of the isoelectronic sequences.

A recently introduced cascade analysis technique is shown to extract reliable lifetimes from heavily cascaded decay curves which are unresolvable by normal curve-fitting techniques. It can also yield information on the relative populations of the excited levels produced in the foil interaction.

The present estimates of silicon in astrophysical objects are not changed by our measurements of transition probabilities in Si II and Si III. The solar photospheric and coronal abundance estimates of silicon relative to hydrogen thus still differ by a factor of three. We have measured the transition probabilities of most of the silicon lines observed in the red-shifted quasar spectra.

1. Introduction

Most of the previous measurements of lifetimes and transition probabilities in silicon have been confined to Si I and Si II. Arc measurements of transition probabilities from relative intensities have been made [1] in Si I and Si II, and Savage and Lawrence [2] have measured some ultraviolet lifetimes. However, there have been many calculations of oscillator strengths in the the lower ionization stages. Most of the earlier results are summarized by Wiese, Smith and Miles [3].

Si III is an interesting example of strong configuration mixing effects which have been carefully studied, in particular, by Zare [6], Weiss [7] and Trefftz [8]. We have made extensive comparisons with their oscillator strengths, and with those for the lower members of this isoelectronic sequence. Zare and Trefftz [9] have compared their results with the Coulomb approximation, and we have already presented some comparisons on the basis of our preliminary measurements [10].

It is important to have experimental verification for the solar and stellar abundances based on these oscillator strengths. Many of the strong lines observed in quasars are resonance transitions in Si II, Si III and Si IV, red-shifted from the vacuum ultraviolet region to visible wavelengths [4]. Rocket spectra of the sun at vacuum ultraviolet wavelengths reveal the same resonance lines [5]. Thus, accurate oscillator strengths for these transitions should help to verify abundances obtained from these transitions.

[1] Present address: Faculté des Sciences, Université de Lyon, 69–Villeurbanne, France.

[2] On leave from the University of Toledo, Toledo, Ohio, USA.

2. Experiment

Doubly and triply charged silicon ions were accelerated to energies of 100–250 keV in an electromagnetic isotope separator, and directed through a thin carbon foil. The light from the foil-excited beam was analyzed at wavelengths between 2 000 and 6 000 Å as described elsewhere [11]. A 1-m vacuum monochromator, equipped with a Bendix Channeltron, detected light at wavelengths below 1 500 Å. The Channeltron was operated in a pulse counting mode with an ELSCINT single channel analyser, which included a ratemeter for direct recording of the spectrum. A sodium salicylate coated EMI 9536 photomultiplier completed our UV detection in the range 1 000–2 500 Å. The lower wavelength cut-off of the grating proved to be about 700 Å. Decay curves were measured as in previous experiments [11].

The doubly-charged silicon isotope of atomic mass 28 was used for the observations above 2 000 Å. The $^{28}Si^{2+}$ was not completely magnetically separated from $^{14}N^{+}$. However, the impurity fraction of nitrogen in the beam was always less than 50% and generally less than 10%. It was noted that the strong N II and N III lines observed above 2 000 Å did not coincide with the strong silicon lines whose decay times were measured. The contrary was true below 2 000 Å, where the N I and N II resonance lines could not be resolved from the Si II, Si III and Si IV resonance transitions. Therefore, the less abundant isotope $^{29}Si^{2+}$ (abundance ratio of 5%) was used for observations using the Channeltron below 1 500 Å. The high detection efficiency enabled us to make decay time measurements using 15–30 nAmp incident beam currents. At such low beam currents, and 150 keV beam energy, foils lasted up to one hour before breaking.

The energy loss of the ions in passing through the foil was measured with a 90° electrostatic analyzer, and calculated from the experimental curves of Fastrup et al. [12] assuming a foil thickness of 10 $\mu g\,cm^{-2}$. The two methods agreed reasonably, and the final ion velocities are known to within 5%. Velocity dispersion of the beam by the carbon foil is calculated to affect the decay times by less than 1%, and can be neglected [13, 14].

3. Results

3.1. *Spectra*

Fig. 1 shows a spectrum of a 140 keV foil-excited silicon beam. Some strong transitions of the first four spectra of silicon are noted. The high yield of Si IV was surprising at these low beam energies, but it indicates that the electrons outside the closed shells isoelectronic to Ne I are easily stripped off and excited in the foil. Thus, Al III and Mg II were the highest easily observable ionization stages previously seen at energies below 160 keV [11]. Similar studies have recently been made with phosphorus,

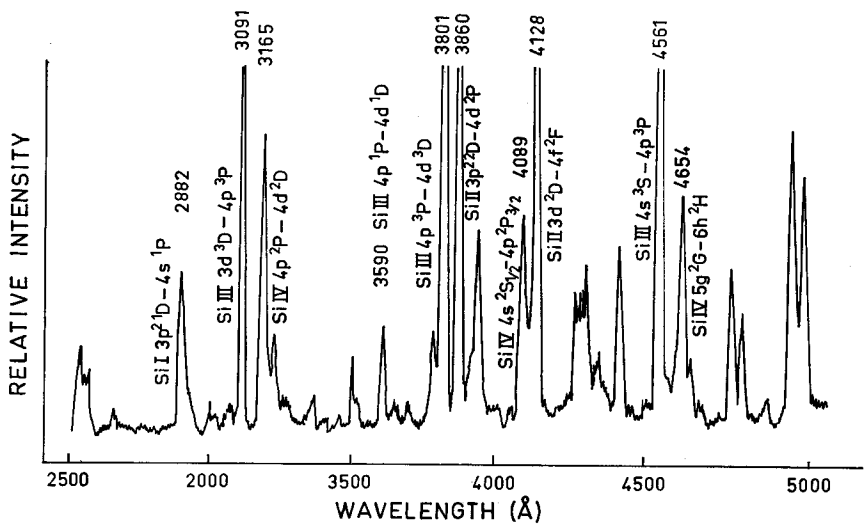

Fig. 1. Spectral scan of foil-excited silicon at 150 keV energy between the wavelengths 2 500 and 5 000 Å.

and accordingly, ionization stages through P V were observed [15]. The $3s$–$3p$ transitions in Si V around 1 200 Å were searched for, but not seen, in the silicon spectra.

A partial spectrum of the vacuum ultraviolet region, detected with the Channeltron is shown in Fig. 2. We observed all the stronger lines of Si II, III and IV in this spectral region, which have been classified by Shenstone [16] and Toresson [17, 18]. The only identified impurity lines observed in the spectra from the foil-excited $^{29}Si^{2+}$ beam came from the carbon foil. In Table I we list these observed lines below 2 000 Å. They include Lyα and Lyβ of hydrogen, and resonance lines of C I, C II, and C III. They are believed to arise from excited atoms and ions ejected from the foil [19].

The lines observed above 2 000 Å could be identified as known Si transitions or nitrogen impurity lines. The only exception was a possible C II transition at 4 265 Å. Few Si I lines [20] were observed and no Si I lifetimes could be measured.

3.2. *Lifetimes—Analysis techniques*

At the Second International Beam-Foil Conference at Lysekil, June 1970, it was accentuated [21] that cascade effects in intensity decay curves can be a major source of error in lifetime measurements. Thus, Wiese [22] emphasized that lifetimes obtained by the Beam-Foil technique show a systematic trend to be higher than theory and other measurements would indicate. Such an increase does result if cascades from longer-lived higher levels are ignored or considered only to a limited extent in the analysis of the decay times. At the same conference, Curtis et al. [23] presented a technique for the elimination of cascade effects by measuring all relevant cascade intensities and decay curves directly, using a detection system whose relative efficiency is known throughout the needed spectral range.

We have since suggested an accuracy parameter, the *Replenishment Ratio* [14] (the ratio of cascade repopulation rate to decay depopulation rate), which is a physically interpretable, mathematical estimate of the amount of cascading in a decay curve. Thus, a replenishment ratio of less than 0.10 is expected to result in a lifetime within 5% of the correct value (assuming no other sources of error).

Since the method discussed in ref. [22] demands accurate knowledge of relative detection efficiencies, we have introduced a new technique which does not require a wavelength calibration of the detection efficiency of the system. The analysis utilizes arbitrarily normalized decay curves of all direct cascades in the analysis of the decay curve of the measured level, and exactly accounts for cascade effects [24].

The ANDC (arbitrarily normalized decay curve) cascade ana-

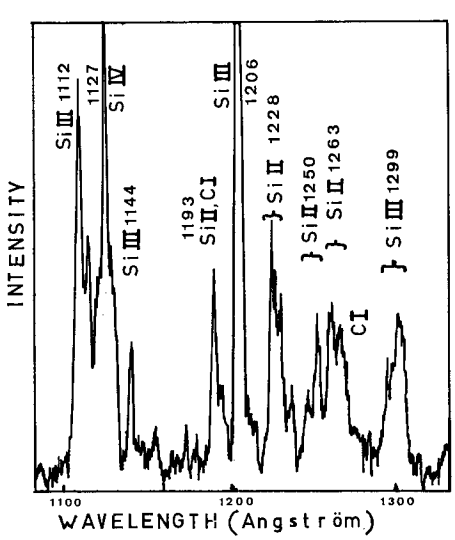

Fig. 2. A partial spectral scan from a foil excited $^{29}Si^{2+}$ beam between 1 100 and 1 300 Å. The decay times of the indicated silicon lines were measured.

Table I. *Lines not classified a silicon transitions observed from a foil-excited $^{29}Si^{2+}$ beam at an incident energy 166 of keV*

Wavelength (Å)	Intensity[a]	Identification	
863±3	10		?
903	16	C II	$2p\ ^2P$–$2p^{22}P$
977	10	C III	$2s^{21}S$–$2p\ ^1P$
1 026	5	H I	$1s\ ^2S$–$3p\ ^2P$
1 117±2	60		?
1 131±2	40		?
1 193	30	Blend C I	$2p^{23}P$–$4d\ ^3D$
1 216	14	H I	$1s\ ^2S$–$2p\ ^2P$
1 236±2	20	Si II	? (1 235.920 Å)[b]
1 278	12	C I	$2p^{23}P$–$3d\ ^3D$
1 335	30	C II	$2p\ ^2P$–$2p^{22}D$
1 463	20	C I	$2p^{21}D$–$3d\ ^1F$
1 560	60	C I	$2p^{23}P$–$2p^{33}D$
1 657	30	C I	$2p^{23}P$–$3s\ ^3P$
1 931	10	C I	$2p^{21}D$–$3s\ ^1P$

[a] Intensities on a linear scale, uncorrected for detection efficiency variations.
[b] An unclassified line attributed to Si II in ref. 16.

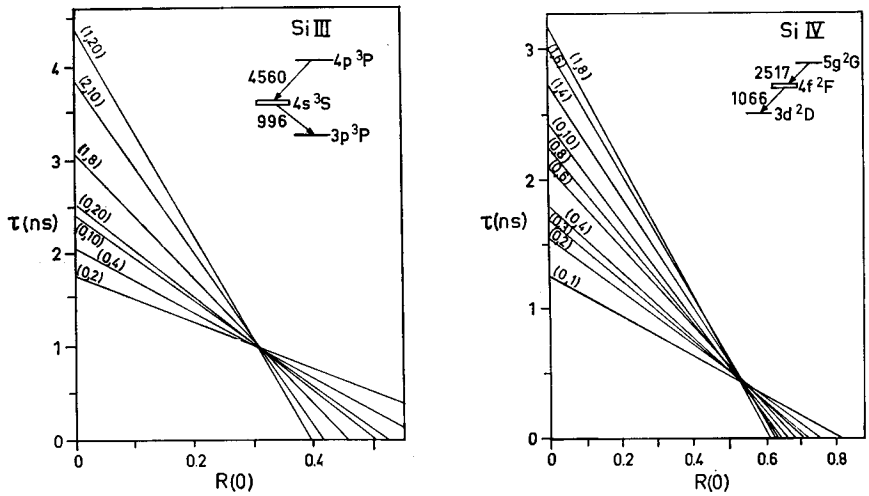

Fig. 3. ANDC cascade analysis. Parametric plots (given by eq. 2) for the decay curves (*a*) Si III, 996 Å, $3p^3P$–$4s^3S$; (*b*) Si IV 1 067 Å, $3d^2D$–$4f^2F$.

lysis can be used to obtain the primary lifetime τ_1 and the replenishment ratio $R(0)$. If we consider a singly cascaded level, and denote by ξ the multiplicative constant which would normalize the cascade ANDC I_2 (t) to the primary ANDC $I_1(t)$, the replenishment ratio is given by

$$R(t) = \xi I_2(t)/I_1(t) \tag{1}$$

We have shown elsewhere [24] that τ_1 and ξ are linearly related by

$$\tau_1 = a(t_I, t_F) - b(t_I, t_F)\xi \tag{2}$$

with

$$a = \int_{t_I}^{t_F} dt\, I_1(t)/[I_1(t_I) - I_1(t_F)] \tag{3}$$

$$b = \int_{t_I}^{t_F} dt\, I_2(t)/[I_1(t_I) - I_1(t_F)] \tag{4}$$

where t_I and t_F are arbitrarily chosen time limits over which the decay curves are to be integrated. A parametric plot of Eq. (2) for a variety of t_I and t_F gives a family of lines, the intersection of which determines the values of τ_1 and $R(0)$. If the cascade transition probability A_{21} is also known, the relative initial populations can be computed, since, for a singly cascaded level

$$N_2(0)/N_1(0) = R(0)/\tau_1 A_{21} \tag{5}$$

This ANDC cascade analysis technique has a number of attractive features. Since the analysis correlates the decay curves of members of a level scheme, a sharp intersection on the plot is strong confirmation that the identifications of the lines are correct, and that the most important cascade has been selected. A diffuse envelope of intersections can indicate that other important cascades have been neglected. In such a case a restricted range of integrations can sometimes be found in which the analyzed cascade dominates, and the intersection becomes sharp. If the ANDC cascade analysis is used in association with traditional curve fitting techniques, it not only offers an alternative check on the primary lifetime and the replenishment ratio, but also implies that the multi-exponential fits of both primary and cascade decay curves should contain the cascade exponential. The ANDC cascade should be more sensitive than a curve fit to short primary lifetimes since it utilizes a stimulus–response relation which persists after the initial population is depleted. This property is valuable in resolving the ambiguity between the cascade and primary exponentials inherent in a "growing-in" decay curve. Most fit analyses have associated the primary lifetime with the fastest exponential which has a positive coefficient, and rejected any growing-in lifetimes as a manifestation of a faster cascade. However, a growing-in can also arise from a slower but more populous cascade (owing to higher statistical weight or selective excitation). As a further check, a correct analysis of a primary decay curve with a non-initial maximum must yield $R(0) > 1$.

We have applied ANDC cascade analysis to those transitions whose major cascade decay curves we also measured. The curves were numerically integrated using a trapezoidal approximation and a linear interpolation was made between measured data points to evaluate a and b for various values of t_I and t_F. In some cases, two cascade decay curves were measured, which both seemed to contribute strongly, as evidenced by diffuse intersections with either ANDC analysis. A three parameter analysis is possible for such cases, but more definitive results were obtained using an alternative two parameter procedure. An "early plot" ($t_I < t_F <$ a few ns from the foil) was made with the faster cascade and a "late plot" (a few ns from the foil $< t_I < t_F$) was made with the slower cascade. If these integration restrictions made both plots intersect sharply at the same value of τ_1 and with a higher $R(0)$ for the faster cascade, then, the analysis was considered valid.

Fig. 3 shows parametric plots obtained for 996 Å Si III, $3p^3P$–$4s^3S$ and for 1 067 Å Si IV, $3d^2D$–$4f^2F$. The scatter in the crossing points gives an indication of the accuracy of the measured lifetimes. In the first case, the result is in good agreement with the lifetime and replenishment ratio obtained from curve fitting, while for 1 067 Å, the ANDC lifetime is half that from curve fitting. None of the results agree with theory. We compare the results from ANDC cascade analysis and from two and three-exponential curve fitting with theory in Table II.

3.3. *Lifetimes—Si II*

The measured Si II decay times are listed in Table III. The decay time of the resonance line at 1 263 Å, $3p^2P$–$3d^2D$, has been obtained from both curve-fitting, and the ANDC technique [24]. The configuration mixing of $3d^2D$ and $3p^{2\,2}D$ is strong, and has been extensively studied theoretically for the Al I isoelectronic sequence [25]. Garstang [26] and Weiss [27] have reviewed the problem and the consequent variations of oscillator strengths along the sequence. Our lifetime value for $3d^2D$ is 50 % higher

Table II. *Comparison of ANDC analysis, curve-fitting, and theoretical lifetimes*

Term[a]	Cascade[b]			ANDC[c]		Fit[d]				
	Early	Full range	Late	$R(0)$	τ_1	$R(0)$	τ_1	τ_2	τ'_2	Theory[e]
Si II										
$3d^2D$(1 265)		$4f\,^2F$(4 128)		0.14	0.47±0.03	0.14	0.45	4.7	4.1	0.33
Si III										
$3d^3D$(1 112)	$4f^3F$(1 501)			0.35	0.55±0.05	0.28	0.36	3.2, 13	2.0, 30	0.36
			$4p^3P$(3 090)	0.23	0.75±0.03				4.1, 24	
$4s\,^3S$(996)		$4p^3P$(4 560)		0.31	1.06±0.02	0.34	0.90	5.0	4.5, 23	0.44
$4f\,^3F$(1 501)		$5g^3G$(4 828)		0.32	1.2 ±0.1	0.16	2.0	30.	4.4, 26	0.48
Si IV										
$3d^2D$(1 128)	$4f\,^2F$(1 067)			0.43	0.48±0.06	0.17	0.85	2.6	0.93, 7	0.38
			$4p^2P$(4 089)	0.22	0.44±0.05				2.3, 0.7, 17	
$4p^2P$(4 089		$4d^2D$(3 165)		1.00	0.75±0.03	1.06	0.65	2.0, 17	2.1, 6.4	0.95
$4f\,^2F$(1 067)		$5g^2G$(2 517)		0.53	0.48±0.04	0.43	0.93	7.0	2.6, 19	0.26
$5g^2G$(2 517)			$6h^2H$(4 654)	0.52	0.65±0.25	0.14	2.6	19.	5.2, 28	

[a] Upper term of the primary decay. The wavelength in Ångströms is given in brackets.
[b] See text for definitions of Early, Full Range and Late.
[c] All lifetimes given in ns.
[d] τ_1 is the primary lifetime, τ_2 the cascade lifetime from the primary decay curve, and τ'_2 the cascade lifetime fitted directly.
[e] Theoretical lifetimes taken from ref. 3, except for the $5g^2G$ term which is the hydrogenic value.

than theory [3], but the same amount lower than the earlier experimental result of Savage and Lawrence [2]. Since both the curve-fitting and ANDC analysis gave the same lifetime value, 0.45 ns, we believe that we have accounted for cascade effects. Other lifetime measurements of $3d^2D$ have been made: in Al I [28] where the configuration mixing is less and agreement with theory is better; and in S IV [29] where blending with a strong S V, transition gave an ambiguous result. The transition $3p^2P$–$3p^{2\,2}D$ at 1 814 Å was too weak in our spectrum to allow a decay time measurement. Froese-Fischer [25] and Weiss [27] have noted that cancellations cause the transition probability to approach zero between Si II and P III. Thus, its intensity should be weak for these elements. Savage and Lawrence [2] give a lifetime for $3p^{2\,2}D$ of 300±100 ns (theory [27]=280 ns) in Si II and Berry et al. [29] measure 7.7±0.5 ns for S IV (theory [27]=16 ns). These results on $3p^{2\,2}D$ and $3d^2D$ indicate that inclusion of configuration interaction has greatly improved the agreement between theory and experiment, but there is still a discrepancy.

The transition observed at 1 228 Å is a blend of two Si II quartet multiplets each expected to be of comparable intensity [16] and of similar lifetime; the multiplet at 1 250 Å could be blended with a Si II doublet transition, but the different fine structure components of the quartet transition can be observed (see Fig. 2). In addition, we note that the intensities of these quartet transitions were comparable to the resonance doublet at 1 253 Å, whereas different intensity patterns were observed in the spark discharge and hollow cathode sources of Shenstone [16]. The doublet transition at 1 250 Å was a factor of 5–10 times weaker than the resonance doublet in Shenstone's spectra. Thus, we have identified the decay time as the lifetime of the $3p^{3\,4}S$ term, which is in reasonable agreement with theory [3].

The unclassified line at 1 236 Å (Table I) had a similar intensity dependence with beam energy as the Si II lines, and is possibly the same unclassified Si II line observed by Shenstone at 1 235.920 Å.

The lifetimes measured in the visible wavelength region agree well with theory [3]. The branching ratios for $4p^2P$ and $4f^2F$ have been taken from theory [3], and have recently been verified experimentally by Schulz-Gulde [31].

Table III. *Si II lifetimes and oscillator strengths*

Wavelength (Å)	Transition	Lifetime τ_1(ns)	Cascade τ_2(ns)	$R(0)$[a]	Absorption oscillator strength[b] This expt.	Theory[c]
1 228	$3p^2\ ^4P$–$3p3d^4P$, $3p^2\ ^4P$–$3p3d^4D$	0.4 ±0.1			—	—
1 250	$3p^2\ ^4P$–$3p^3\ ^4S$	0.35±0.1	1.8	0.22	0.22	0.29
1 263	$3p\ ^2P$–$3d\ ^2D$	0.45±0.05[d]	4.7	0.14	0.88	1.2
3 858	$3p^2\ ^2D$–$4p\ ^2P$	8.3±0.8	—	—	0.046	0.038
6 355	$4s\ ^2S$–$4p\ ^2P$	—	—	—	1.5	1.26
4 130	$3d\ ^2D$–$4f\ ^2F$	4.1 ±0.4	9.9	0.11	0.52	0.51
2 072	$3p^2\ ^2D$–$4f\ ^2F$	—	—	—	0.093	0.092
5 200	$3p4p^4D$–$3p4d^4P$	5.0 ±1			—	—

[a] The Replenishment Ratio, defined in the text.
[b] The branching ratios from ref. 3 have been used to calculate the oscillator strengths from $4p^2P$ and $4f^2F$.
[c] Wiese, Smith and Miles [3]. The values are from unpublished calculations of A. W. Weiss.
[d] Savage and Lawrence [2] obtained a lifetime of 0.7±0.2 ns from this transition.

3.4. *Lifetimes—Si III*

Si III, as a member of the Mg I isoelectronic sequence, is a two electron spectrum for which the displaced term system ($3pnl$) mixes configurations with the normal term system ($3sn'l'$). Zare [6] and Trefftz [8] have included configuration interaction in their calculations using two different methods, and they have compared their resulting oscillator strengths with two different Coulomb approximations [9]. The configuration interaction is so strong that the identity of a term in the single configuration picture is sometimes in doubt [9]. This is particularly true for the singlets as initially pointed out by Toresson [17]. For the stronger transitions, the results of Trefftz and Zare [9] are in good agreement with each other and with the calculation of Weiss [7] which also include configuration interaction.

Table IV compares our lifetimes results with theory. No other measurements of these lifetimes have been made. The decay of the resonance transition $3s^1S$–$3p^1P$ at 1 207 Å is shown in Fig. 4, together with the relevant cascades into $3p^1P$. The decay is decomposed into two exponentials with lifetimes of 0.40 ns and 13 ns, the fast decay being in good agreement with the theoretical lifetime of 0.39 ns for the $3p^1P$ term. However, this agreement may be coincidental as there are many cascades and

Table IV. *Si III lifetimes and oscillator strengths*

Wavelength (Å)	Transition	Lifetime τ_1 (ns)	Cascade τ_2 (ns)	$R(0)$	Theor. NBS[a]	lifetime Z, T^b (ns)	Absorption oscillator strength Expt.	Theory[b]
968	$3p^2\,^1D$–$5f\,^1F$	1.0±0.5	—	—	—	0.77[c]	0.092	0.12
996	$3p\,^3P$–$4s\,^3S$	1.06±0.05	5.0	0.31	0.42	0.44	0.048	0.11
1 112	$3p\,^3P$–$3d\,^3D$	0.36±0.04	3.2, 13	0.28	0.35	0.36	0.87	0.86
1 207	$3s\,^1S$–$3p\,^1P$	0.40±0.1	13	0.04	0.39	0.39	1.7	1.66
1 299	$3p\,^3P$–$3p^2\,^3P$	0.34±0.1	1.4, 15	0.13	0.45	0.47	0.74	0.55
1 501	$3d\,^3D$–$4f\,^3F$	1.2 ±0.1[d]	30	0.32	—	0.48[c]	0.42	0.97
2 542	$3p\,^1P$–$3p^2\,^1D$	26 ±3	—	—	31	28, 56	0.06	0.06[e]
3 090	$3d\,^3D$–$4p\,^3P$	4.1 ±0.5	24	0.04	—	3.6[c]	0.12[f]	0.14
3 487	$4d\,^3D$–$5f\,^3F$	1.4 ±0.2	8.	0.15	—	0.92[c]	0.27	0.40
3 590	$4p\,^1P$–$4d\,^1D$	1.9±0.3	—	—	—	0.93[c]	0.45	0.91
3 801	$4p\,^3P$–$4d\,^3D$	4.0 ±0.4	40	0.03	2.4	2.8[c]	0.80	1.2
3 924	$4f\,^1F$–$5g\,^1G$	4.1 ±0.4	9.5	0.20	—	2.4[g]	—	—
4 561	$4s\,^3S$–$4p\,^3P$	4.5 ±0.5	23	0.03	—	3.6[c]	0.92[f]	1.1
4 822	$4f\,^3F$–$5g\,^3G$	4.3 ±0.5	26	0.33	—	3.6[g]	—	—

[a] Ref. 3, earlier theoretical values.
[b] An average (see text) of calculations in ref. 9. Two values are quoted where the values are very different.
[c] Other possible branching modes have been taken into account.
[d] Result obtained also from ANDC cascade analysis.
[e] From Zare [6].
[f] Assumed lifetime is the average of those measured at 3 090 and 4 561 Å.
[g] Hydrogenic values.

blends associated with this transition. The $3d\,^1D$ term has a theoretical lifetime of 0.20 ns, and its decay to $3p\,^1P$ at 1 207 Å is too close in wavelength to be resolved from the resonance line. It was hoped to resolve it in terms of a growing-in cascade. However, none was observed, and it most probably was not within our time resolution. The transitions to $3p\,^1P$ from $4s\,^1S$ at 1 312 Å, from $3p^2\,^1S$ at 1 417 Å, and from $4d\,^1D$ at 823 Å were observed to be weak in intensity, and have decay times similar to the $3p\,^1P$ term [9]. Two cascades could be measured directly: the $4d\,^1D$ lifetime of 1.9 ns measured by its transition to $4p\,^1P$ at 3 590 Å is twice that of theory [9]; while the $3p^2\,^1D$ term has a measured lifetime of 26 ns in close agreement with the calculations of Zare and Weiss but not with those of Trefftz.

Additional blending can occur through the decays to $3p^2\,^1D$ from $3d'\,^1D$ at 1 208 Å and $4f\,^1F$ at 1 210 Å. The latter was semi-resolved from the 1 207 Å line, but blended with a Si IV transition and is estimated to be less than 10% of the total intensity at 1 207 Å. In addition, the transitions should have decay times of less than 1 ns, with little resulting effect on the main decay. In view of the above complications, a two exponential fit to the $3p\,^1P$ decay is clearly inadequate. Most of the cascades were too weak to be measured directly, which made it impossible to apply the ANDC cascade analysis technique. However, the replenishment ratio from the observed cascade is very low, and thus the evaluated lifetime should be reliable.

The ANDC cascade analysis was applied to decays for a number of triplet terms, and the results were generally in good agreement with theory. An exception is the $4s\,^3S$ term. We obtain the same lifetime from curve-fitting and ANDC for the transition $3p\,^3P$–$4s\,^3S$ at 997 Å which is twice the theoretical value. The cascading in this case is simple, and no blending is suspected. The cascade decay time was constant over more than one decade of the decay. Also, it agrees with the lifetime of the $4p\,^3P$ term measured directly at 3 090 and 4 561 Å to $3d\,^3D$ and $4d\,^3S$ respectively. From the three values, we estimate the lifetime of the $4p\,^3P$ term to be 4.3 ±0.4 ns.

The oscillator strength for the transition $3p\,^3P$–$4s\,^3S$ is shown in Fig. 5 for the first few members of the Mg I isoelectronic sequence. It indicates large differences between experiment and theory.

The oscillator strengths for the other triplet transitions are shown in Fig. 6. The $3p\,^3P$–$3d\,^3D$ transition shows good agreement between theory and experiment while the $3p\,^3P$–$3p^2\,^3P$ transition shows an unusual example of the experimental f-values being significantly higher than theory.

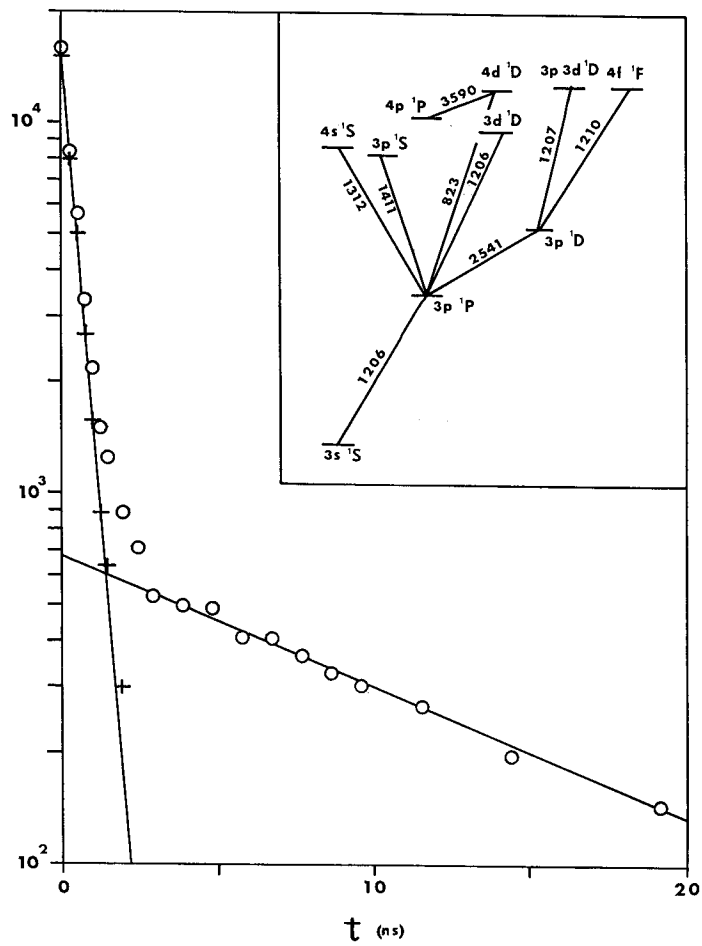

Fig. 4. Intensity decay curve of Si III, 1 206 Å, $3s\,^1S$–$3p\,^1P$. The inset shows most of the blends and cascades which contribute to this decay.

Table V. *Si IV lifetimes and oscillator strengths*

Wavelength (Å)	Transition	Lifetime τ_1 (ns)	Cascade τ_2 (ns)	$R(0)$	Theor. lifetime[a] (ns)	Absorption oscillator strength Expt.	Theory[a]
1 067	$3d^2D$–$4f^2F$	0.48±0.04[b]	7.0	0.5	0.26	0.50	0.93
1 128	$3p^2P$–$3d^2D$	0.46±0.05[b]	2.6, 14	0.33	0.38	0.70	0.84
1 397	$3s^2S$–$3p^2P$	1.2 ±0.4	0.3[e], 6	3.0	1.09	0.73	0.80
2 517	$4f^2F$–$5g^2G$	2.6 ±0.3	19	0.14	1.0[c]		
3 165	$4p^2P$–$4d^2D$	2.1 ±0.2	6.4	0.22	1.74[d]	0.99	1.19
3 766	$4d^2D$–$5p^2P$	2.2 ±0.2	0.7[e], 16	0.81	1.33[d]	0.18	0.30
4 089	$4s^2S$–$4p^2P$	0.75±0.03[b]	2.0, 17	1.06	0.95[d]	1.48	1.17
4 654	$5g^2G$–$6h^2H$	5.2 ±0.5	28	0.33	2.4[c]		

[a] Ref. 3. Self consistent field calculations or Coulomb approximation.
[b] Obtained from ANDC cascade analysis; $\tau_1, \Delta\tau_2, R(0)$ from ANDC (early and late averaged), τ_2 from primary fit.
[c] Hydrogenic value.
[d] Other branching modes have been taken into account.
[e] Growing-in cascade.

3.5. *Lifetimes—Si IV*

As a single electron spectrum of the sodium sequence, the theoretical values for the transition probabilities are expected to be quite accurate [3]. However, Table IV indicates that our measurements show some quite large differences from theory. The ANDC cascade analysis has been used extensively in obtaining the results, and in some cases yields lifetimes which differ substantially from those obtained by curve fitting. In such single electron spectra, the limited branching and greater statistical weight of the highest orbital angular momentum term of a given principal quantum number often cause severe cascading to the nearest lower term. Thus, inclusion of this single cascade is often sufficient for reliable ANDC analysis.

The lifetimes of the first three ^2P terms were measured. The resonance transition $3s^2S$–$3p^2P$ at 1 1397 Å, the $4p^2P$ was measured via the $4s^2S$ branch at 4 088 Å, and the $5p^2P$ was measured via the $4d^2D$ branch at 3 762 Å. All three of these terms had fast growing-in exponentials in their decay curves, and interpretation requires careful consideration of the cascade contributions.

The curve fitted lifetime of the $3p^2P$ term was barely in agreement with theory [3], but the experimental values of the oscillator strengths for this transition in the isoelectronic sequence mostly fall below theory, as shown in Fig. 7. It is uncertain whether the difference is real, or is due to incomplete resolution of the cascading in the curve fits. ANDC analysis of the $3p^2P$ term with the measured nd^2D cascades gave diffuse intersections, implying that there were also strong cascades from the ns^2S terms, and the 0.3 ±0.1 ns growing-in exponential is

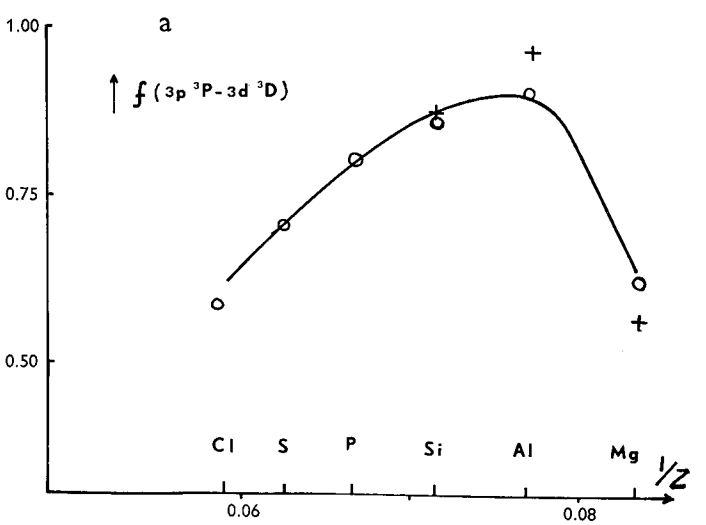

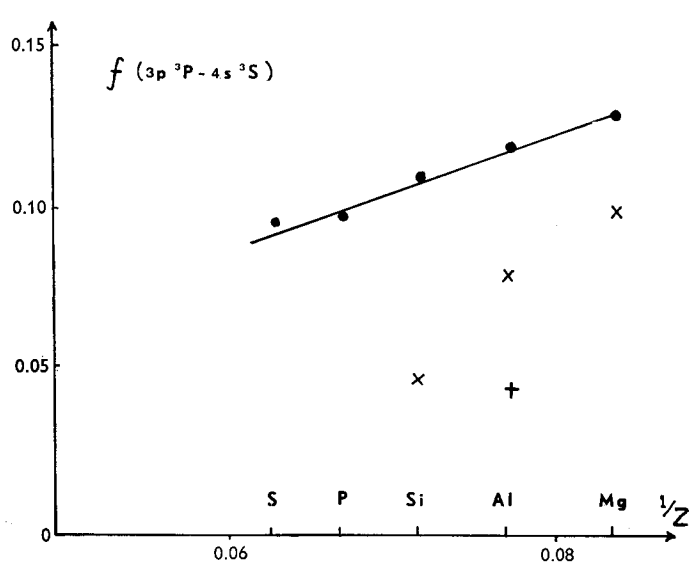

Fig. 5. Oscillator strength versus Z^{-1} for $3p^3P$–$4s^2S$ in the Mg I isoelectronic sequence. The theoretical values (●) are from ref. 3, and the experimental values (×) from ref. 11. The result (+) for Al II is from ref. 28.

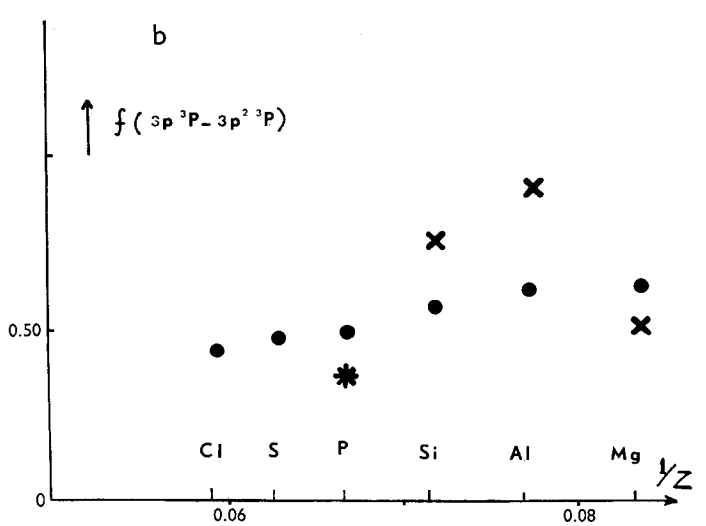

Fig. 6. Oscillator strengths in the Mg I isoelectronic sequence: (*a*) $3p^3P$–$3d^3D$ and (*b*) $3p^3P$–$3p^{23}P$. The theoretical values (●, ○) are from ref. 3, and the experimental values (×, +) from refs. 11 and 28. The experimental value for phosphorus (*) is from recent work of Curtis and Martinson.

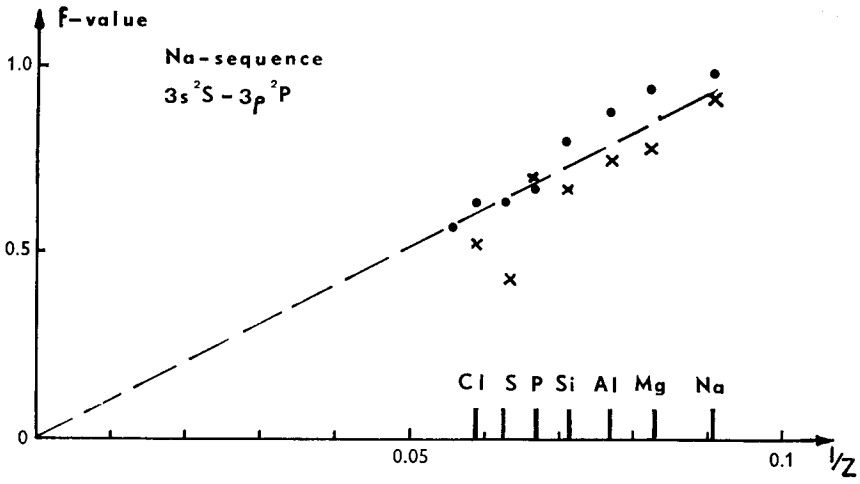

Fig. 7. Oscillator strength versus Z^{-1} for $3s^2S$–$3p^2P$ in the Na I isoelectronic sequence. The theoretical values (●) are from ref. 3 and the experimental values (×) from refs. 11, 28 and 29, 15. The experimental value for phosphorus (×) is from recent work of Curtis and Martinson.

interpreted as a result of fast cascades from the $4s^2S$, $3s^2S$ and $3d^2D$ terms.

The growing-in exponentials in the $4p^2P$ and $5p^2P$ decay curves were fit to values of 0.6 ± 0.2 and 0.7 ± 0.3 ns. Thus, these exponentials could be attributed to fast cascades from the $5s^2S$ and $6s^2S$ terms, which have theoretical lifetimes of 0.48 and 0.77 ns [3]. However, an ANDC cascade analysis of $4p^2P$ with its cascade from $4d^2D$ yielded a sharp intersection, with a primary lifetime corresponding to the growing-in, and a replenishment ratio of unity. This seems to imply that the $4p^2P$ growing-in is actually a result of repopulation of the fast primary level by a slower but more populous cascade from $4d^2D$, and $5s^2S$ cascade effects are negligible. No cascades were measured in the case of the $5p^2P$, so ANDC analysis could not be used to resolve the ambiguity in assignment.

Three cascades into the $3d^2D$ were measured, from $4p^2P$, $5p^2P$, and $4f^2F$. ANDC analysis gave a sharp "early plot" intersection with $4f^2F$, and a sharp "late plot" intersection with $4p^2P$, both at the same value of primary lifetime, and with replenishment ratios which verified that the $4f^2F$ is initially stronger. The ANDC lifetime value is half that obtained by curve fitting, and slightly longer than the theoretical value. Only the cascade of lower angular momentum was measured for the $4d^2D$, and a very diffuse ANDC intersection implied there was other stronger cascading.

The ANDC analysis of the $4f^2F$ lifetime yields a value which is, again, half the value obtained by curve fitting, but is a factor of two longer than the theoretical value. The ANDC analysis of the $5g^2G$ term yielded an intersection which shifted smoothly between early and late plots, but did not achieve a range of constancy, so the term must be strongly affected by cascades throughout the measured region. However, the envelope of primary lifetimes traced out is well below the curve fit lifetime.

4. Conclusion

Our agreement with previous values for transition probabilities for Si II transitions at visible wavelengths [3] indicates that solar abundance estimates for the photosphere based in these lines [32, 30] are unchanged. Lambert and Warner [30] have demonstrated the consistences of abundances obtained from the Si I abundance determinations [33, 34] based on the same transitions

Pottasch [36, 37] has determined the coronal abundance of silicon from the resonance transitions of Si III and Si IV. Our measured *f*-values for these transitions are in good agreement with those used by Pottasch. Thus, the abundance of silicon relative to hydrogen appears to be a factor of three higher in the corona than in the photosphere. This factor is the same for the neighbouring element phosphorus, but slightly lower (2 and 2.5 respectively) for aluminium and magnesium [32].

We conclude that the theoretical calculations of oscillator strengths including configuration interaction are reliable for the strong transitions of Si III, but errors up to 50% may be present in some of the weaker transitions. In Si II and Si IV the transition probabilities given by Wiese, Smith and Miles [3] are generally in good agreement with our experimental values. Exceptions are the $3d^2D$ term in Si II, where configuration interaction is considerable, and some of the higher excited terms in Si IV.

We find that straightforward fitting of cascade-affected decay curves by two or more exponentials can lead to erroneous results for lifetimes in error by up to 100%. Considerably improved accuracy has been obtained by including multi-exponential decays from directly observed cascades in our analysis.

5. Acknowledgements

We thank I. Martinson for many helpful discussions and for his critical reading of the manuscript.

Two of us (H G. B. and L. J. C.) are grateful for all the Swedish hospitality shown during our stay in Stockholm. Professor Ingmar Bergström's interest and the technical help of L. Lundin and J. Hilke were essential in the completion of the experiment. Financial support from the Swedish Natural Science Research Council is gratefully acknowledged.

References

1. Hey, P., Z. Physik **157**, 79 (1959).
2. Savage, B. D. and Lawrence, G. M., Ap. J. **146**, 940 (1966).
3. Wiese, W. L., Smith, M. W. and Miles, B. M., Atomic Transition Probabilities, vol. II. NSRDS — Nat. Bur. Std. 22. Washington, D.C., 1969.
4. Burbridge, E. M., Ap. J. **149**, L51 (1967); C. R. Lynds, Proceedings of 1st BFS Conference. Beam Foil Spectroscopy (ed. S. Bashkin). Gordon & Breach, New York, 1968.
5. Detwiler, C. R., Garret, D. L., Purcell, J. D. and Tousey, R., Ann. Géophys. **17**, 263 (1961).
6. Zare, R. N., J. Chem. Phys. **47**, 3561 (1967).
7. Weiss, A. W., J. Chem. Phys. **47**, 3573 (1967).
8. Friedrich, H., and Trefftz, E., J. Quant. Spect. and Rad. Transf. **9**, 333 (1969).
9. Trefftz, E. and Zare, R. N. J. Quant. Spect. and Rad. Transf. **9**, 643 (1969).
10. Bromander, J., Berry, H. G. and Buchta, R., Nucl. Inst. and Meths. **90**, 55 (1970).

11. Berry, H. G., Bromander, J. and Buchta, R. Physica Scripta **1**, 181 (1970).
12. Fastrup, B., Hvelplund, P. and Sautter, C. A., Mat. Fys. Medd. Dan. Vid. Selsk. **35**, 10 (1966).
13. Högberg, G. Nordén, H. and Berry, H. G., Nucl. Inst. and Meths. **90**, 283 (1970).
14. Curtis, L. J., Berry, H. G. and Bromander, J., Physica Scripta **2**, 216 (1970).
15. Martinson, I., Private communication.
16. Shenstone, A. G., Proc. Roy. Soc. **261A**, 153 (1961).
17. Toresson, Y. G., Arkiv Fysik **18**, 389 (1960).
18. Toresson, Y. G., Arkiv Fysik **17**, 179 (1960).
19. Berry, H. G., Martinson, I. and Bromander, J., Phys. Letters **31A**, 521 (1970).
20. Radziemski, L. J., Jr and Andrew, K. L., J. Opt. Soc. Am. **55**, 467 (1965).
21. Nucl. Inst. and Meths. **90**, section V, p. 173 (1970).
22. Wiese, W. L., Nucl. Inst. and Meths. **90**, 25 (1970).
23. Curtis, L. J., Schectman, R. M., Kohl, J. L., Chojnacki, D. A. and Shoffstall, D. R., Nucl. Inst. and Meths. **90**, 217 (1970).
24. Curtis, L. J., Berry, H. G. and Bromander, J., Phys. Letters **34A**, 169 (1971).
25. Froese-Fischer, C., Ap. J. **151**, 759 (1968).
26. Garstang, R. H., Proceedings of 1st BFS Conference. Beam Foil Spectroscopy (ed. S. Bashkin). Gordon & Breach, New York, 1968.
27. Weiss, A. W., Nucl. Inst. and Meths. **90**, 121 (1970).
28. Andersen, T., Jessen, K. A. and Sørensen, G., J. Opt. Soc. Am. **59**, 1197 (1969).
29. Berry, H. G., Schectman, R. M., Martinson, I., Bickel, W. S. and Bashkin, S., J. Opt. Soc. Am. **60**, 335 (1970).
30. Lambert, D. L. and Warner, B., Mon. Not. Roy. Ast. Soc. **138**, 213 (1968).
31. Schulz-Gulde, E., J. Quant. Spect. and Rad. Transf. **9**, 13 (1969).
32. Engvold, O. and Hauge, Ö., Nucl. Inst. and Meths. **90**, 351 (1970).
33. Searle, L. and Sargent, W. L. W., Ap. J. **139**, 787 (1964).
34. Auer, L. H., Mihalas, D., Aller, L. H. and Ross, J. E., Ap. J. **145**, 153 (1966).
35. Hinteregger, H. E., J. Geophys. Res. **66**, 2367 (1961).
36. Pottasch, S. R., Ap. J. **137**, 945 (1963).
37. Pottasch, S. R., Sp. Sc. Rev. **3**, 816 (1964).

Research Institute for Physics
S-104 05 Stockholm 50
Sweden